

Scattering volume dependence on the electron density in the collective Thomson scattering using gyrotron for ECH

ECH用ジャイロトロンを用いた協同トムソン散乱計測における 散乱体積の密度依存性

S. Kubo^{1,2)}, M. Nishiura³⁾, K. Tanaka¹⁾, T. Shimozuma¹⁾, Y. Yoshimura¹⁾, H. Igami¹⁾, H. Takahashi¹⁾, T. Ii¹⁾, Ogasawara Shinya³⁾, R. Makino³⁾, K. Kobayashi³⁾, Y. Goto³⁾

¹⁾National Institute for Fusion Science, 322-6 Oroshi-cho, Toki 509-5292, Japan

²⁾Grad. School of Frontier Sciences, The University of Tokyo, 5-1-5 Kashiwanoha, Chiba, 277-8561, Japan ³⁾Dept. of Energy Science and Technology, Nagoya Univ., Nagoya 464-8463, Japan

¹⁾核融合科学研究所 〒 509-5292 岐阜県土岐市下石町 322-6

²⁾ 東京大学大学院新領域創成科基盤科学研究系先端エネルギー工学専攻 〒 277-8561 千葉県 柏市 柏の葉 5-1-5

³⁾ 名古屋大学大学院工学研究科エネルギー理工学専攻 〒 464-8463 名古屋市千種区不老町

Collective Thomson scattering measurement has been realized in the magnetic fusion confinement machines utilizing the recent development of high power gyrotrons. To extend this method, the confirmation of the scattering volume is important in both defining the spatial resolution and discriminating the real scattered signal from stray radiation. The beam scan experiments have been performed in LHD plasmas scanning the receiving antenna during discharges. It is found that the clear scattering volume effect appears above background scattering signals. The effective scattering volume calculation code from ray tracing result for both probing and receiving beams is developed and compared with the experimental results.

1. Introduction

Collective Thomson scattering (CTS) is one of the promising methods to directly measure the ion distribution function in the high temperature and high density fusion plasma. Due to its small crosssection, high power probe beam and highly sensitive receiver are required for CTS. Recent development of high power gyrotron for the electron cyclotron resonance heating (ECRH) enlarged a scattering signal above detectable level. Accompanied with the gyrotron development and wide applications of its power, high performance transmission line and antenna system are also developed for ECRH. It is reasonable to utilize such developed ECRH system for CTS. CTS has been tried in LHD using 77 GHz 1 MW gyrotron and attaching heterodyne receiver on one of the ECRH transmission line. One of the specific features of CTS is the high spatial resolution which can be defined by a cross-section of probing and receiving beam. It is important to confirm that the scattering signal level increases as the scattering volume. The beam scan experiment is described in section 2. These results are compared with a newly developed effective scattering volume estimation in section 3.

2. Beam Scan Experiment

The fast scanning mirror is set at one of the antenna system in LHD. The CTS receiver attached to this line enabled to scan the receiving beam in time during a discharge. Probing beam from 77 GHz 1MW gyrotron is fixed in position but 100 % square wave power modulated at 50 Hz to dis-

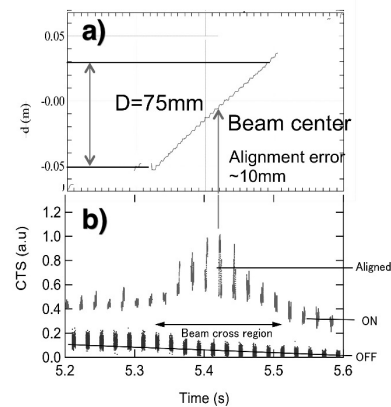


Fig. 1 Typical beam scan results. a) Time trace of the distance between vacuum beam axis. b) Scattering signal intensity

criminate background ECE. The receiving antenna angle is scanned so that the receiving beam scans from outside to inside and again outside in time. In Fig.1 a) is shown the distances of beam axis in time, and the scattering volume peak was expected to occur at $t=5.4$ s, but actual received signal reaches maximum at $t=5.42$ s as shown Fig.1 b). Since the probing beam is 100% modulated at 50 Hz, it is clear that the scattering component dominates the received signal. The width is as almost expected from vacuum Gaussian beam optics, but the volume center shifted by 10 mm. This shift is almost the order of setting error of

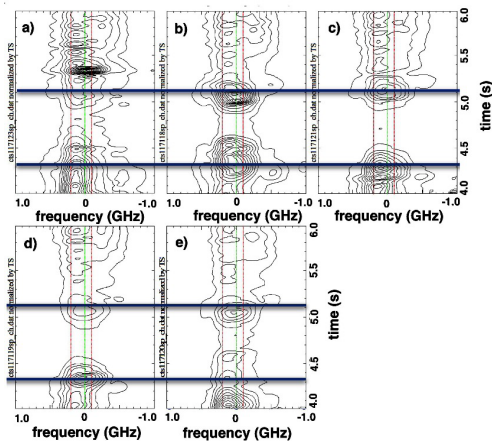


Fig. 2 Contour plot of the time dependent frequency spectra for a)1.3, b)1.5-1.7, c)1.6, d)1.7-1.9 e) $1.9-2.0 \times 10^{19} \text{ m}^{-3}$. Thick long lines indicate the timings when the scattering volume is expected to have maximum for vacuum condition.

the beam alignment. So, it can be concluded that the both injection and receiving beams are well defined.

Similar CTS beam scan experiments are repeated for several target plasma density ranging from 1.3 to $2.0 \times 10^{19} \text{ m}^{-3}$. In this series of experiments the receiving antenna scan sequence is fixed for every shot so that the vacuum receiving beam axis is scanned from outside to inside and back to outside and crosses vacuum probing beam axis at $t=4.3$ and 5.2 s. Fig.2 show the contour of the time evolution of CTS spectra for the various density. Here the background ECE and background scattering signal are subtracted. Although the peak intensity varies a little in time and in shot, the peak position in time almost coincide with the time when the expected vacuum beam crosses. The beam peak position tends to shift a little outward as the density increased, although the probing and receiving beam deflection effect should not be negligible near the density of $2.0 \times 10^{19} \text{ m}^{-3}$. This suggests that the both probing and receiving beam deflects appreciably but in the same direction and the both deflected beam crossed near the antenna angle at which the vacuum beams crosses.

3. Scattering volume estimation from raytracing calculation

Since the antenna system in LHD adopted quasi-optical highly focussed beam, the method to estimate the effective scattering volume taking both the distribution of the probing beam power and that of receiving antenna sensitivity into account have been developed [2] assuming both Gaussian beam distribution. This method is extended to the results of multi-raytracing for finite density to apply to high density plasmas where the deflection effect is not negligible. Ray tracing code calculates multi-rays propagate independently using geometrical optics. Gaussian beam is simulated by

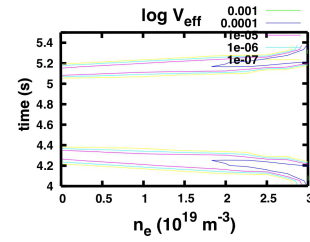


Fig. 3 The dependence of the effective scattering volume on density as the beam scanned in time same as the beam scan experiment.

multi rays whose intensities are weighted as the original Gaussian distribution and assumed that the beam power flux passing through the cross section surrounded by the points the rays pass through are kept constant. Both probing and receiving beams are simulated with this method and effective scattering volume is calculated by summing up all the crossing volume with the multiplied weights of both probing and receiving ray segments. Such calculation is repeated for the simulated probing and receiving beam position as the series of density scan experiment discussed in section 2. Fig.3 shows the estimated density dependences of the scattering volume. Both experimental results and those of raytracing found to coincide with each other fairly well in the density region below $1.5 \times 10^{19} \text{ m}^{-3}$. As discussed in section 2, even with the distance over 15cm, scattering signal still remains. Moreover the spectrum shape at such zero scattering volume condition is narrower but similar and has no spetial non-thermal wave feature. This suggests that the origin of the background scattering signal is from the reflection at the opposite side of the wall along the same observation path through the scattering volume. Collective Thomson scattering can occur at any point of the probing high power beam pass through inside the plasma. Such scattered radiation should have CTS spectrum shape reflecting the plasma parameter there and can contaminate as the reflection from opposite side of the wall.

4. Conclusions

CTS signal observed in LHD is confirmed to dominantly contain the CTS radiation from scattering volume in relatively wide range of electron density. But also contains multi reflection component of CTS which possibly comes from the probing beam path but not from scattering volume. A method to estimate the effective scattering volume is developed utilizing the Gaussian weighted multi-raytracing of both proving and receiving beam.

Acknowledgement

This work was supported by JSPS KAKENHI Grant Number 24360385 and National Institute for Fusion Science under ULRR701 and ULRR804.

- [1] S. Kubo *et al.*, RSI **81** (2010) 10D535.
- [2] S. Kubo *et al.*, PFR **5** (2010) S1038.
- [3] M. Nishiura *et al.*, NF **54** (2014) 023006.